Rev. Adv. Mater. Sci. 34 (2013) 12-18

HIGHLY DISCLINATED GRAPHENE

I.A. Ovid'ko[1,2]

[1] Department of Mathematics and Mechanics, St. Petersburg State University, St. Petersburg 198504, Russia
[2] Institute of Problems of Mechanical Engineering, Russian Academy of Sciences, Bolshoj 61, Vasilievskii Ostrov, St. Petersburg 199178, Russia

Received: May 8, 2013

Abstract. Graphene with a high-density ensemble of homogeneously dispersed topological disclinations is defined and theoretically described as a new two-dimensional material hereinafter called highly disclinated graphene (HDG). Within the suggested approach, positive and negative disclinations – pentagon and heptagon rings – in hexagonal lattice of graphene create the nanoscopically buckled structure containing local "hills" and "valleys". It is theoretically shown that the buckled structure is responsible for non-linear superelasticity of graphene-HDG nanocomposites and may cause other, potentially excellent mechanical characteristics of such nanocomposites and HDG.

1. INTRODUCTION

Graphene - a monolayer with the hexagonal sp^2 covalently bonded crystal structure - represents the subject of explosively growing interest in physics and materials science due to its unique mechanical, electron transport and thermal properties; see, e.g., reviews [1-4] and papers [5-14]. In particular, two-dimensional (2D) graphene is specified by superior intrinsic strength of ≈130 GPa and extremely high Young modulus (in-plane stiffness) of ≈1.0 TPa [5]. At the same time, pristine graphene can be easily rolled due to its 2D flat geometry and material properties. With this behavioral feature, graphene represents a mature material for carbon nanotubes resulted from rolling of graphene ribbons [1,10]. Also, out-of-plane bending/buckling can come into play in 2D graphene sheets due to their elastic straining by external mechanical load [14-18] and/or the presence of internal defects like topological and grain boundary disclinations [10,19-21]. In doing so, local curvature of buckled graphene sheets significantly or even crucially influences their electronic properties [15-17,22-25]. More than that, with curvature produced by defects, graphene can serve as a mature material for other curved carbon allotropes [10,19-21]. For instance, graphene sheets can be globally (but not only locally) curved when they contain positive and negative topological disclinations - pentagon and heptagon rings, respectively - in hexagonal crystal lattice (Fig. 1). So, insertion of positive topological and negative disclinations into a mature graphene sheet with hexagonal crystal lattice and associated bending produce various curved carbon nanostructures (e.g., cones, capped carbon nanotubes, fullerenes, etc.), whose geometries depend on the number and location of these topological disclinations [10,19-21]. Also, dipoles of closely distant positive and negative topological disclinations – pentagon-heptagon pairs – represent topological dislocations which are typical defects in graphene [21,26-28]. In this situation, curvature associated with positive disclination of a dipole configuration is compensated by curvature created by negative disclination of the dipole, and a dislocated graphene is flat on average. In particular, dipoles of closely distant topological disclinations play the role of basic structural blocks

Corresponding author: I.A. Ovid'ko, e-mail: ovidko@nano.ipme.ru

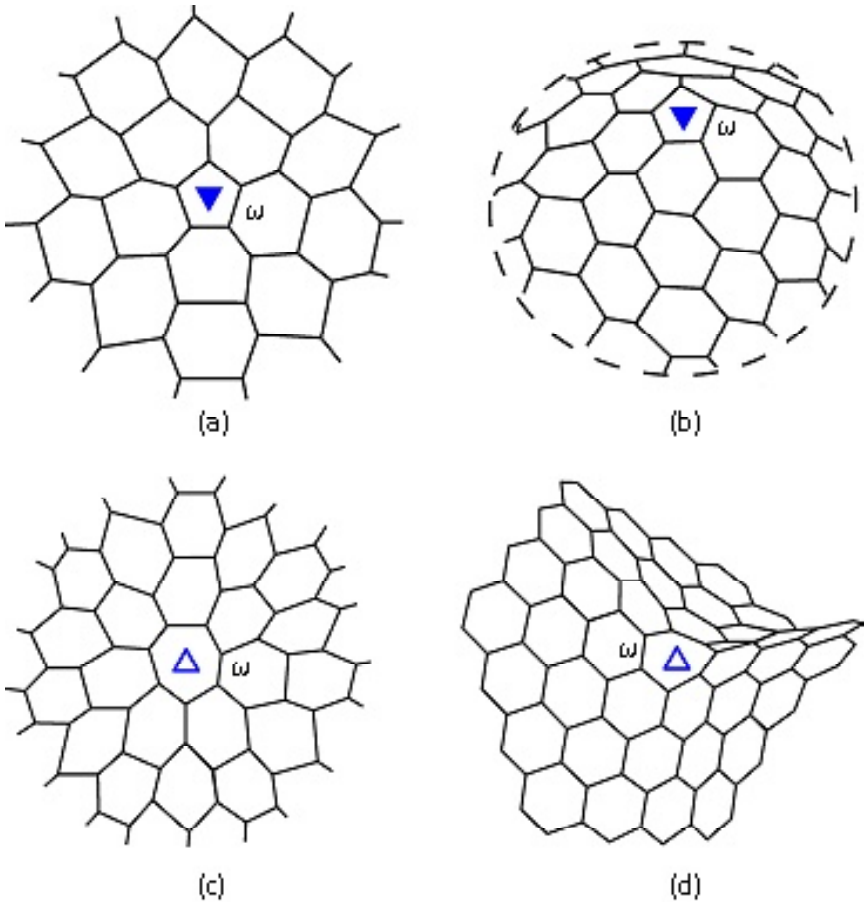

Fig. 1. (color online) Topological disclinations with strengths $\omega = \pm\pi/3$ in hexagonal crystal lattice of graphene. (a) Positive disclination of strength $\pi/3$ (pentagon marked by full triangle) in a flat graphene membrane creates high in-plane distortions and stresses. (b) A free-standing graphene membrane with a positive disclination transforms into a curved cone structure having blunt top. (c) Negative disclination of strength $-\pi/3$ (heptagon marked by open triangle) in a flat graphene membrane creates high in-plane distortions and stresses. (d) A free-standing graphene membrane with a negative disclination transforms into a into saddle-like structure.

of grain boundaries in graphene [4,21,27-32]. In these cases, the distance *L'* between topological disclinations composing dipole configurations (or, in other terms, topological dislocations) is of the atomic scale: $L' \leq a$, with *a* being the crystal lattice parameter [21,27-32].

The main aim of this paper is to predict and theoretically describe a new carbon material (allotrope), the namely HDG defined here as a free-standing graphene that contains a high-density ensemble of homogeneously dispersed positive and negative topological disclinations with a *nanoscopic* mean distance *L* between neighboring disclinations. In this special carbon allotrope, the characteristic distance *L* is in the range: $200a \geq L \geq 2a$. We will theoretically examine the structural features of HDG and graphene-HDG nanocomposites as well as estimate some of their mechanical properties.

2. GEOMETRY AND ENERGY CHARACTERISTICS OF INDIVIDUAL TOPOLOGICAL DISCLINATIONS IN GRAPHENE

First, let us briefly discuss geometry of individual topological disclinations in graphene. Typical positive and negative topological disclinations in graphene with hexagonal crystal lattice are pentagons and heptagons (Fig. 1) characterized by disclination strengths $\omega = \pi/3$ and $-\pi/3$, respectively; for details, see, e.g., Refs. [19,21,27,28]. Insertion of a sole positive or negative topological disclination into a free-standing graphene sheet creates high in-plane stresses which can effectively relax through its buckling that transforms the sheet into a cone-like or saddle-like carbon structure, respectively (Fig. 1). Following the general theory of free-standing

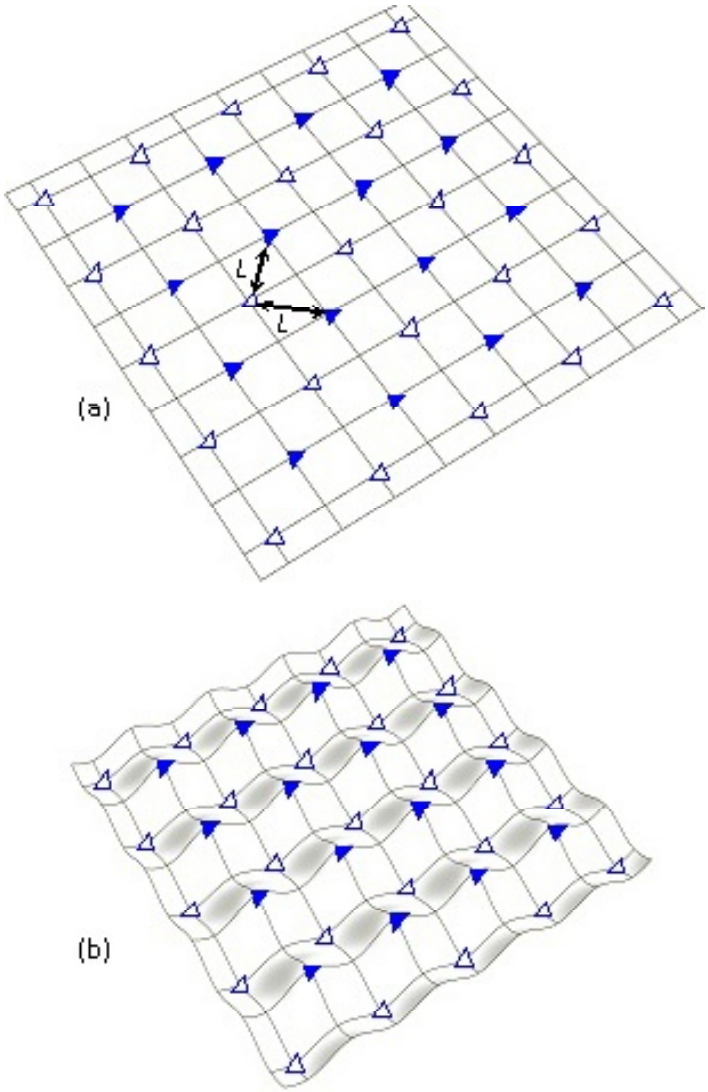

Fig. 2. (color online) Geometric features of highly disclinated graphene (HDG). HDG represents a free-standing graphene with positive and negative topological disclinations (full and open triangles, respectively) arranged in a periodic superlattice. (a) Flat state. (b) Buckled state. Positive and negative topological disclinations correspond to local hills and valleys, respectively.

membranes/sheets containing sole disclinations [33], the buckling process is controlled by balance between the bending and stretching energies. Below we will consider this balance in graphene.

The energy E_f of a sole disclination located in center of a circle-like flat membrane is as follows [33]:

$$E_f = Y\omega^2 R^2 / 32\pi. \quad (1)$$

Here Y is the Young modulus, ω is the disclination strength, and R is the membrane radius. The energy E_b of a disclination located in center of a buckled membrane is given as [33]:

$$E_b = \beta k |\omega| \ln(R/a). \quad (2)$$

Here k denotes the bending rigidity, R the radius of the membrane in its flat state, a the lattice spacing, and β the factor taking into account the disclination type ($\beta = 3.456/\pi$ and $= 7.545/\pi$, for positive and negative disclination, respectively).

In order to compare the energies E_f and E_b of disclinated graphene membranes, we exploit the following typical values of graphene parameters: Y = 1 TPa [5], $\omega = \pm \pi/3$, $k = 2.31\ 10^{-19}$ N m [34]. With these values, one finds that E_f is by several orders larger that E_c, for any $R \geq a$. Thus, the buckled state of disclinated graphene membranes is always

energetically favorable ($E_f >> E_c$) over their flat state.

3. GEOMETRY AND ENERGY CHARACTERISTICS OF PERFECT HDG

Now let us consider the specific structural and geometric features of a perfect HDG defined here as a free-standing graphene with positive and negative topological disclinations arranged in a periodic superlattice with period L. The perfect HDG in its flat and buckled states is schematically presented in Fig. 2. Each positive (negative, respectively) disclination in the perfect HDG is surrounded by its negative (positive, respectively) neighboring counterparts (Fig. 2). In this case, after some analysis based on the theory of disclinations in solids [35-37], we find the following. The stress field created by a disclination - pentagon or heptagon - is effectively screened by its neighboring counterparts on the distance $r \approx L/2$ from the disclination (by analogy with the stress field of a disclination in a circle-like membrane of radius $L/2$, in which the screening effect is provided by the membrane free surface). The screening effect gradually decreases down to around zero when r diminishes from $L/2$ down to $L/4$. In the area specified by $r \le L/4$, the stress field of the disclination is very weakly affected by its neighboring disclinations. As a result, each disclination in HDG (Fig. 2) creates the stress field which is very similar to that created by a disclination of the same type in a graphene membrane free from other disclinations (Fig. 1). Then, in a first approximation, the specific strain energy W (per unit area) of a perfect HDG sheet can be represented as the sum of specific strain energies (per unit area) of its constituent disclinations each being located in a circle-like membrane of radius $\approx L/2$. That is, $W = W_f \approx (1/S)\Sigma(E_f)_i \approx (1/L^2)Y\omega^2 L^2/128\pi$, if the HDG specimen is flat (Fig. 2 a), or $W = W_b \approx (1/S)\Sigma(E_b)_i \approx (1/L^2)\ 5.5\ k|\omega|ln(L/2a)/\pi$, if the HDG specimen is buckled and contains hills and valleys associated with its disclinations (Fig. 2b). Here S is the area of the HDG specimen; Σ means the summation over all the disclinations of the HDG specimen; $(E_f)_i$ and $(E_b)_i$ are the energies of the ith disclination in the circle-like graphene membrane in its flat and buckled states, respectively; and L^2 is the HDG area per one disclination. With formulas (1) and (2) giving the strain energies of disclinated graphene membranes in its flat and buckled states, respectively, for the previously specified values of graphene parameters, one finds the following inequality:

$$W_f \approx Y\pi/1152 >> W_b \approx \left(\frac{1}{L^2}\right)1.833k\ln\left(\frac{L}{2a}\right), \quad (3)$$

for any $L \ge a$.

According to inequality (3), the buckled state of HDG (Fig. 2b) is always (for any $L \ge a$) energetically favorable ($W_b << W_f$) over its flat state (Fig. 2a), as with the case of graphene membranes containing sole disclinations (Fig. 1). This statement is well consistent with both experimental observations and computer simulations of carbon nanostructures containing individual disclinations and their groups; see, e.g., papers [19,21,38] and references therein.

4. HDG STRUCTURES

We considered the model situation with the perfect HDG. In general, in real situations, HDG specimens having various structures can exist which are briefly as follows: (i) HDG with an *approximately periodic* (non-perfect) superlattice or even *highly disordered* arrangement of topological disclinations in the situation where numbers of positive and negative topological disclinations are identical. In doing so, though a HDG specimen is nanoscopically buckled, it is flat on the mesoscale level specified by the length $\lambda \ge 10L$. (ii) HDG with positive and negative topological disclinations whose numbers are different. In this case, a HDG specimen is characterized by non-zero sum disclination strength, and thereby it is curved on the mesoscale level. In the context discussed, by analogy with curved carbon nanostructures that can be fabricated from mature polycrystalline graphene through engineering of GB disclinations [21], there is a technologically attractive and scientifically significant opportunity to generate curved carbon nanostructures with various geometries/shapes through engineering of topological disclinations in HDG. (iii) "Structural" graphene-HDG nanocomposite with graphene matrix and HDG inclusions being nanoscale disclination configurations; see, e.g., Fig. 3. These HDG inclusions are analogs of second-phase nanoparticles in conventional nanocomposites. A scientifically interesting example of such graphene-HDG nanocomposites is represented by a graphene specimen with nanoscale disclination quadrupoles (HDG inclusions) arranged in superlattice, as it is schematically illustrated in Figs. 3a and 3b.

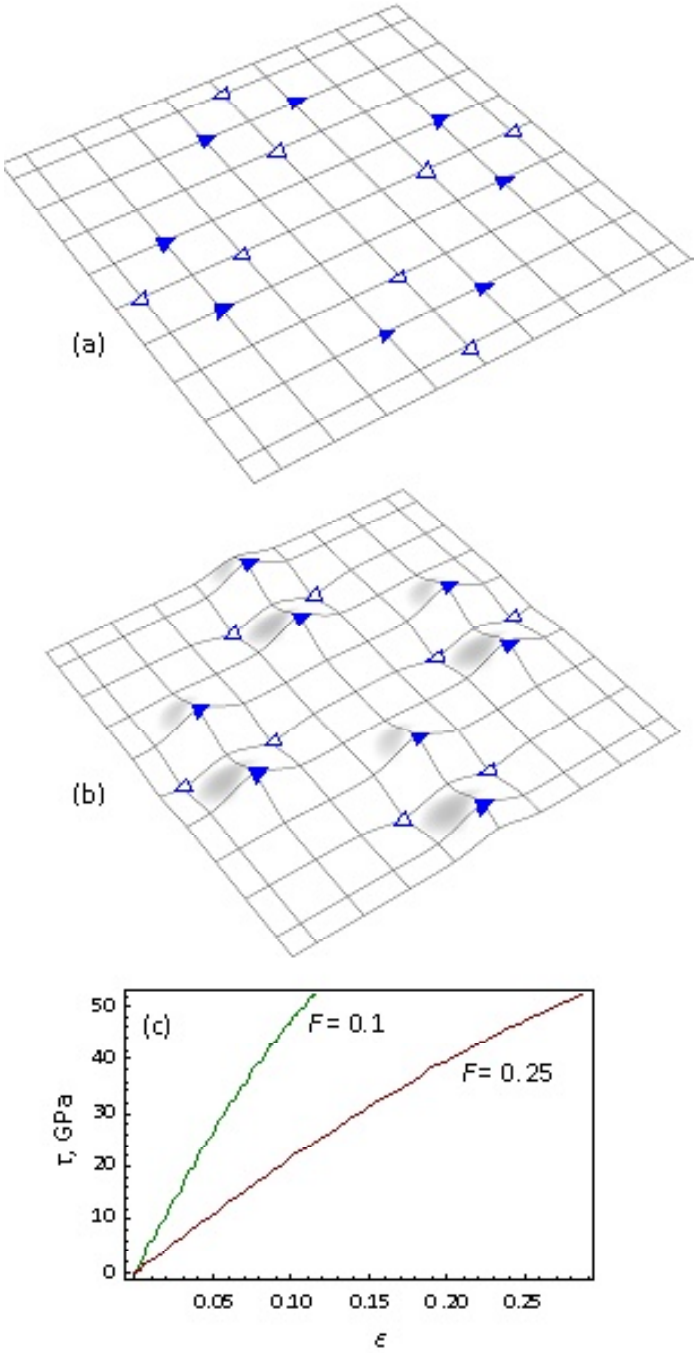

Fig. 3. (color online) Geometry and stress-strain dependences for "structural" graphene-HDG nanocomposite with graphene matrix and HDG inclusions being nanoscale disclination quadrupoles. (a) Flat and (b) buckled states of nanocomposite. (c) Stress-strain (τ-ε) dependences in the elastic deformation test.

Disclination quadrupoles are chosen because they represent minimal HDG units that, according to the disclination theory [35-37], do not create long-range stress fields. Besides, by analogy with disclination quadrupoles and their constituent elements – disclination dipoles - in 3D nanomaterials [39-43], they may serve as effective carriers of plastic flow in HDG.

5. ELASTIC DEFORMATION OF GRAPHENE-HDG NANOCOMPOSITE

Let us consider elastic deformation of a graphene-HDG nanocomposite (Fig. 3). Note that its buckled/corrugated state (Fig. 3b) is energetically preferred, as with perfect HDG. Due to corrugations, linear

sizes of the buckled specimen (Fig. 3b) are lower than those of its flat counterpart (Fig. 3a). Elastic deformation of the buckled nanocomposite (Fig. 3b) can significantly extend it through diminishing its local curvature. In doing so, the bending energy initially accumulated in local hills and valleys of the nanocomposite is transformed into its stretching energy in parallel with both increase in strain (and linear sizes of the specimen) and decrease in heights of hills and valleys.

After some algebra based on the disclination theory (see, e.g., Refs. [35-37]), we calculated the stress–strain dependence for a graphene-HDG nanocomposite in the elastic deformation test in which the initially buckled nanocomposite (Fig. 3b) becomes approximately flat (Fig. 3a). In this case, for definiteness, we considered *square* disclination quadrupoles as HDG inclusions in the nanocomposite under uniaxial tensile load. The calculated stress-strain dependence is approximately given as:

$$\tau = FY\left[\arctan\left(\varepsilon / 2F\right)\right]^2 \ln 2 / \pi\varepsilon. \qquad (4)$$

Here τ is the external shear stress needed to provide the flattening process (Figs. 3a and 3b), ε is the corresponding elastic strain (ε ranges from 0 to $2F\tan(\pi/6)$), and F is the area fraction occupied by the disclination quadrupoles. In the case of Y = 1 TPa, for F = 0.1 and 0.25, the calculated stress-strain dependences are presented in Fig. 3 c. In general, in the range of F = 0.1 – 0.25, we find $\varepsilon \approx$ 10 – 30%. These are very high values indicative of superelastic behavior of graphene-HDG nanocomposites.

Pristine graphene or graphene sheets containing low densities of defects typically exhibit brittle behavior without any plastic deformation. At the same time, there are experimental data [44,45] indicating on dislocation-carried plasticity of graphene in the situations where either lattice dislocation dipoles are generated under electron irradiation or lattice dislocations pre-exist in graphene as structural blocks of grain boundaries that move/migrate. That is, plastic deformation carried by lattice dislocations can occur in graphene in certain conditions. Since disclinations serve as sources and sinks of dislocations in solids [35-37,46], it is logical to think that the disclinated structure of HDG can enhance plastic flow. More precisely, emission of dislocations from disclinations, motion of these dislocations in graphene and their absorption by other disclinations can effectively provide plastic flow in HDG and graphene-HDG nanocomposites.

In contrast to pristine graphene, HDG is expected to exhibit high resistance to rolling. It is because, for geometric reasons, the rolling of HDG leads to a partial flattening of hills and valleys associated with its disclinations. This rolling process is followed by the reverse buckling-to-stretching energy transformations which hamper the process in HDG.

6. CONCLUDING REMARKS

Thus, HDG and graphene-HDG nanocomposites serve as special 2D materials having the specific structural features: they contain high-density ensembles of topological disclinations and show pronounced nanoscopic buckling which creates local hills and valleys associated with disclinations (Figs. 2 and 3). Following our theoretical estimates, these structural features can lead to enhanced mechanical properties (superelasticity, good plasticity at elevated temperatures and/or electron beam irradiation, and high resistance to rolling) of HDG and graphene-HDG nanocomposites.

ACKNOWLEDGEMENTS

The work was supported, in part, by the Russian Ministry of Education and Science (Contract No 8025), St. Petersburg State University research grant 6.37.671.2013, and the Russian Foundation of Basic Research (grant 12-01-00291-a).

REFERENCES

[1] A.K. Geim and K.S. Novoselov // *Nature Mater*. **6** (2007) 183.
[2] A.H. Castro Nero, F. Guinea, N.M.R. Peres, K.S. Novoselov and A.K. Geim // *Rev. Mod. Phys*. **81** (2009) 109.
[3] A. A. Balandin // *Nature Mater*. **10** (2011) 569.
[4] I.A. Ovid'ko // *Rev. Adv. Mater. Sci*. **34** (2013) 1.
[5] C. Lee, X. Wei, J.W. Kysar and J. Hone // *Science* **321** (2008) 385.
[6] G.D. Lee, C.Z. Wang, E. Yoon, N.M. Hwang, D.-Y. Kim and K.M. Ho // *Phys. Rev. Lett.* **95** (2005) 205501.
[7] E. Miniussi, M. Pozzo, A. Baraldi, E. Vesselli, R.R. Zhan, G. Comelli, T.O. Menteş, M.A. Niño, A. Locatelli, S. Lizzit and D. Alfè // *Phys. Rev. Lett.* **106** (2011) 216101.
[8] M.M. Ugeda, D. Fernández-Torre, I. Brihuega, P. Pou, A.J. Martínez-Galera, Rubén Pérez and J. M. Gómez-Rodríguez // *Phys. Rev. Lett.* **107** (2011) 116803.

[9] Y. Kim, J. Ihm, E. Yoon and G.D. Lee // *Phys. Rev.* B **84** (2011) 075445.
[10] S. Gupta and A. Saxena // *J. Appl. Phys*. **109** (2011) 074316; **112** (2012) 114316.
[11] T. Low, V. Perebeinos, J. Tersoff and Ph. Avouris // *Phys. Rev. Lett.* **108** (2012) 096601.
[12] P. T. Araujo, D. L. Mafra, K. Sato, R. Saito, J. Kong and M. S. Dresselhaus // *Phys. Rev. Lett.* **109** (2012) 046801.
[13] D. A. Abanin and D. A. Pesin // *Phys. Rev. Lett.* **109** (2012) 066802.
[14] B. Liu, C.D. Reddy, J. Jiang, J.A. Baimova, S.V. Dmitriev, A.A. Nazarov and K. Zhou // *Appl. Phys. Lett.* **101** (2012) 211909.
[15] N. Levy, S.A. Burke, K.L. Meaker, M. Panlasigui, A. Zettl, F. Guinea, A.H. Castro Neto and M.F. Grommie // *Science* **329** (2010) 544.
[16] T. Georgiou, L. Britnell, P. Blake, R.V. Gorbachev, A. Gholinia, A.K. Geim, C. Casiraghi and K.S. Novoselov // *Appl. Phys. Lett.* **99** (2011) 093103.
[17] J.A. Baimova, S.V. Dmitriev and K. Zhou // *Phys. Status Solidi B* **249** (2012) 1393.
[18] B. Liu, C.D. Reddy, J. Jiang, J.A. Baimova, S.V. Dmitriev, A.A. Nazarov and K. Zhou // *Phys. Rev. B* **101** (2012) 211909.
[19] S. Ihara, S. Itoh, K. Akagi, R. Tamura and M. Tsukada // *Phys. Rev. B* **54** (1996) 14713.
[20] S. Gupta and A. Saxena // *J. Raman Spectroscopy* **40** (2009) 1127.
[21] I.A. Ovid'ko // *Rev. Adv. Mater. Sci*. **30** (2012) 201.
[22] V.M. Pereira and A.H. Castro Neto // *Phys. Rev. Lett.* **103** (2009) 046801.
[23] V. Atanasov and A. Saxena // *Phys. Rev. B* **81** (2010) 205409.
[24] V. Atanasov and A. Saxena // *J. Phys.: Condens. Matter* **23** (2011) 175301.
[25] F. Guinea, M.I. Katsnelson and A.K. Geim // *Nature Phys.* **6** (2011) 30.
[26] A. Hashimoto, K. Suenaga, A. Gloter, K. Urita and S. Ijima // *Nature* **430** (2004) 870.
[27] O.V. Yazyev and S. Louie // *Phys. Rev. B* **81** (2010) 195420; *Nature Mater*. **9** (2010) 806.
[28] Y. Liu and B.I. Yakobson // *Nano Lett*. **10** (2010) 2178.
[29] O. V. Yazyev and S. Louie // *Nature Mater*. **9** (2010) 806.
[30] P. Kim // *Nature Mater*. **9** (2010) 792.
[31] K. Kim, Z. Lee, W. Regan, C. Kisielowski, M. F. Gommie and A. Zettl // *ACS Nano* **5** (2011) 2142.
[32] P.Y. Huang, C.S. Ruiz-Vargas, A.M. van der Zande, W.S. Whitney, M.P. Levendorf, J.W. Kevek, S. Garg, J.S. Alden, C.J. Hustedt, Y. Zhu, J. Park, P.L. McEuen and D.A. Muller // *Nature* **469** (2011) 389.
[33] H.S. Seung and D.R. Nelson // *Phys. Rev. A* **38** (1988) 1005.
[34] Y. Wei, B. Wang, J. Wu, R. Yang and M.L. Dunn // *Nano Lett.* **13** (2013) 26.
[35] A.E. Romanov and V.I. Vladimirov, In: *Dislocations in Solids*, edited by F.R.N. Nabarro, North-Holland Publ. Co., Amsterdam (1992). Vol. 9, pp. 191–302.
[36] M.Yu. Gutkin and I.A. Ovid'ko, *Plastic Deformation in Nanocrystalline Materials,* Springer, Berlin, New York, etc. (2004).
[37] M. Kleman and J. Friedel // *Rev. Mod. Phys*. **80** (2008) 61.
[38] A. Krishnan, E. Dujardin, M.M.J. Treacy, J. Hugdahl, S. Lynum and T.W. Ebbesen // *Nature* **388** (1997) 451.
[39] I.A. Ovid'ko // *Science* **295** (2002) 2386.
[40] C.C. Koch, I.A. Ovid'ko, S. Seal and S. Veprek, *Structural Nanocrystalline Materials: Fundamentals and Applications* (Cambridge University Press, Cambridge, 2007).
[41] S.V. Bobylev and I.A. Ovid'ko // Appl. Phys. Lett. **92**, 081914 (2008).
[42] S.V. Bobylev, N.F. Morozov and I.A. Ovid'ko // *Phys. Rev. Lett*. **105** (2010) 055504; *Phys. Rev. B* **84** (2011) 094103.
[43] N.F. Morozov, I.A. Ovid'ko and N.V. Skiba // *Rev. Adv. Mater. Sci*. **29** (2011) 180.
[44] J.H. Warner, E.R. Margine, M. Mukai, A.W. Robertson, F. Guistino and A.I. Kirkland // *Science* **337** (2012) 209.
[45] S. Kurasch, J. Kotakowski, O. Lehtinen, V. Skakalova, J. Smet, C.E. Krill III, A.V. Krasheninnikov and U. Kaiser // *Nano Lett*. **12** (2012) 3168.
[46] M.Y. Gutkin, I.A. Ovid'ko and N.V. Skiba // Mater. Sci. Eng. A **339** (2003) 73.